Novel Assembled Sensorized Glove Platform for Comprehensive Hand Function Assessment by Using Inertial Sensors and Force Sensing Resistors

Bor-Shing Lin, *Member, IEEE*, I-Jung Lee, *Graduate Student Member, IEEE*, and Jean-Lon Chen

***Abstract*—This study proposed a novel assembled sensorized glove combining nine-axis inertial measurement units (IMUs) and force sensing resistors (FSRs) to simultaneously measure hand kinematics and fingertip force. The sensorized glove was designed to have high flexibility and extensibility. The accuracy and reliability of the hand kinematics measurements were verified using four-finger flexion–extension tasks. The results reveal that the mean absolute errors (MAEs) of the joint angles of fingers are all <5°, thus indicating that the glove can precisely measure hand kinematics. The MAE of the fingertip force prediction was 1.47 N, thus revealing that the FSRs can accurately measure the fingertip force. Moreover, comprehensive evaluation was conducted to prove that the sensorized glove can not only simultaneously measure the hand kinematics and fingertip force but also distinguish between the subjects with distinct hand functions. Therefore, the sensorized glove proposed in this study is reliable and has a strong potential for application in practical rehabilitation settings.**

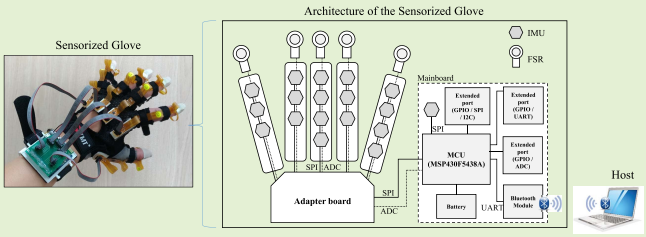

***Index Terms*—Force sensors, hand function assessment, hand kinematics, inertial measurement units, sensorized gloves.**

I. Introduction

HAND function is usually considered the comprehensive performance of manual dexterity and fingertip force [1]–[4]. Hand function assessment is essential for hand rehabilitation to evaluate the recovery of hand function impairment. Measuring hand kinematics [5]–[6] and fingertip force [4] for further evaluation are two important processes when conducting hand function assessment. By measuring hand kinematics and fingertip force, physicians can keep a track of the recovery progress of patients' hand function impairment in an objective manner. To improve the quality of hand function assessment and reduce the burden on physicians, various studies for automatically capturing hand kinematics or fingertip force have been proposed in recent years.

The studies for capturing hand kinematics can be divided into two categories: optical-based [7]–[8] and sensor-based [5], [6], [9]–[15] systems. In the studies including optical-based systems, optical markers have been used to track the positions of a user's hand, and users do not have to wear any devices. However, occlusion and time-consuming calibration are the primary disadvantages of optical-based systems. Therefore, some studies indicated that using sensor-based systems is more practical than using optical-based systems [16]. The sensors in these sensor-based systems mainly include bend sensors [5], [9]–[10] and inertial measurement units (IMUs) [6], [11]–[15]. However, the bend sensors can only

Manuscript received November 1, 2019; revised December 5, 2019; accepted December 5, 2019. Date of publication December 10, 2019; date of current version February 14, 2020. This work was supported in part by the Ministry of Science and Technology in Taiwan under Grant MOST 107-2221-E-305-014 and Grant MOST 108-2314-B-305-001, in part by the University System of Taipei Joint Research Program under Grant USTP-NTPU-TMU-108-01, and in part by the Faculty Group Research Funding Sponsorship by National Taipei University under Grant 2019-NTPU-ORDA-03. The associate editor coordinating the review of this article and approving it for publication was Prof. Subhas C. Mukhopadhyay. *(Corresponding author: Bor-Shing Lin.)*

B.-S. Lin is with the Department of Computer Science and Information Engineering, National Taipei University, New Taipei City 23741, Taiwan (e-mail: bslin@mail.ntpu.edu.tw).

I-J. Lee is with the Department of Computer Science and Information Engineering, National Taipei University, New Taipei City 23741, Taiwan, and also with the College of Electrical Engineering and Computer Science, National Taipei University, New Taipei City 23741, Taiwan (e-mail: akino_sumiko@hotmail.com).

J.-L. Chen is with the Department of Physical Medicine and Rehabilitation, Chang Gung Memorial Hospital, Chang Gung University, Taoyuan City 33378, Taiwan, and also with the Medical Department, Medical College, Chang Gung University, Taoyuan 33302, Taiwan (e-mail: bigmac1479@gmail.com).

Digital Object Identifier 10.1109/JSEN.2019.2958533

measure rough joint angles, and the calibration process of bend sensors is time-consuming. Moreover, most bend sensors have low linearity, and it is difficult to obtain an absolute joint angle in every situation by using these sensors. Therefore, IMUs have become a superior solution for measuring human kinematics. Several IMU-based sensorized gloves have been proposed to date. In 2014, Kortier *et al.* proposed a sensorized glove to capture hand kinematics [6]. The advantage of this study is that it used three IMUs that is worn on the back of the hand to create a robust hand model. Moreover, several experiments were conducted to validate the system's reliability. However, the glove system used a wired universal serial bus (USB) connection, which might be a potential limitation in the clinical usage. In 2016, Choi *et al.*proposed a glove embedded with 17 inertial sensors [11]. This system can measure Euler angles in three directions. However, the sensor board that must be worn on the back of the hand is bulky. Moreover, the use of only one sensor to represent the movement of the back of the hand may lead to inaccuracy when measuring the kinematics of the metacarpophalangeal (MCP) joint. In 2017, Fang *et al.* proposed a glove platform that can track the motion of the left or right hand [12]. However, the study only measured the Euler angles but did not measure the value of the joint angles, which is important in clinical setting. In 2018, Connolly *et al.* proposed a sensorized glove for patients with arthritis [13]. The sensorized glove used a combination of printed circuit boards (PCBs) and stretchable PCBs to construct a flexible glove. However, the PCB that must be worn on the back of the hand is bulky and heavy for patients and causes inconvenience when conducting hand movement. To address the issue, in 2018, Lin *et al.* proposed a data glove with nine-axis inertial sensors [14]. This data glove combines the advantages of PCBs and flexible PCBs. However, this study did not conduct a three-dimensional (3D) verification of joint angles. The PCBs attached to the finger segments might be slightly heavy for patients. In 2019, Salchow-Hömmen *et al.* proposed a sensorized glove to solve the problems in the aforementioned study [15]. IMUs were soldered on the flexible PCBs to make them light and flexible. Several experiments were conducted to validate the reliability of the system. However, as in the study by Kortier *et al.* [6], the sensorized glove used a wired USB connection, which is a limitation for use in the clinical environment.

Although the techniques for measuring hand kinematics are well developed and can be applied to many fields, the techniques cannot provide the fingertip force. To measure the fingertip force, several studies have combined motion sensors with force sensing sensors to measure the hand kinematics and fingertip force [17]–[19]. In 2015, Hsiao *et al.* developed a data glove with nine-axis IMUs and force sensing resistors (FSRs) [17]. To the best of our knowledge, the study is the first one to combine IMUs with FSRs to simultaneously obtain hand kinematics and fingertip force. The aim of this study was to implement the system prototype and prove that IMUs and FSRs could be combined. Therefore, this study did not completely validate the reliability and accuracy of the joint angles and fingertip force. Moreover, the FSRs adopted in this study were not linear; thus, accurate force measurement cannot be obtained using these FSRs. In 2016, Kortier *et al.* proposed a system combining the previous designed data glove with force sensors [18]. The system quantified the interaction between a finger and the object that the finger pinched. However, the force sensor used in this study is bulky and might not applicable to delicate rehabilitation tasks. In 2017, Liu *et al.* proposed a glove-based system that combines the IMUs with six Velostat force sensors to study the hand–object manipulation [19]. The force sensor used in this study is lighter than that adopted in the study by Kortier *et al*. and can obtain the force distribution of the entire hand. However, same as the study by Hsiao *et al.* [17], the study by Liu *et al*. [19] did not validate the reliability and accuracy of measuring hand kinematics and force. Based on a literature survey, it can be concluded that the technology of simultaneously capturing hand kinematics and fingertip force were available but still not well developed. Therefore, it is necessary to construct a system that can solve the aforementioned limitations.

The aforementioned limitations are listed as follows. First, most designs could not be extended, so they could not communicate with other biomedical sensors. Second, these sensorized gloves may not fit both left and right hands. Third, these sensorized gloves did not evaluate the accuracy of finger joint angle measurement in a 3D situation. Finally, although sensorized gloves for hand kinematics measurement were well developed, their combination with fingertip force measurement was still not available or not well developed. However, fingertip force is also a critical criterion for hand function assessment [1]–[3].

To overcome the aforementioned issues, a novel assembled sensorized glove combining nine-axis IMUs and FSRs was developed in this study. The sensorized glove can provide both kinematic data and fingertip force to physicians. The extended ports on the main board can provide several interfaces, including serial peripheral interface (SPI), inter-integrated circuit (I2C), universal asynchronous receiver/transmitter (UART), analog-to-digital converter (ADC), general-purpose input/output (GPIO). In future studies, the extended ports can be used to connect various sensors. Several experiments were also conducted to ensure the reliability of the system. The novel glove system can eliminate the limitations of previous studies and can be used as a robust tool by physicians to assess patients' hand functions.

II. Hardware Design

Fig. 1 shows the overview of the proposed sensorized glove system. Each data glove comprises 18 IMUs (MPU9250, InvenSense, San Jose, CA, USA). The sensorized glove collects the raw data from the 18 IMUs when the subject is conducting the tasks for hand function assessment. After collecting the data from the IMUs, the data are immediately transmitted to the evaluation program via Bluetooth (HL-MD08R-C2-AT, Hotlife, Taipei, Taiwan) or UART. The evaluation program derives the acceleration, angular rate, and magnetic field values from the raw data. Moreover, the joint angle between every two adjacent finger segments

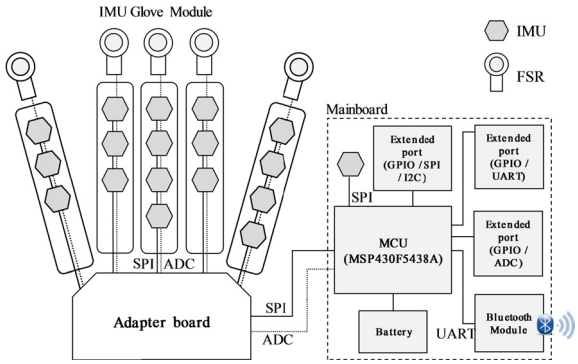

Fig. 1. Architecture of the proposed sensorized glove.

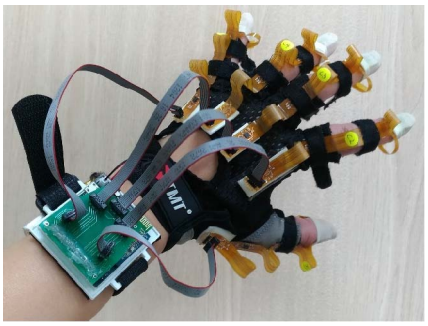

Fig. 2. Prototype of the nine-axis sensorized glove.

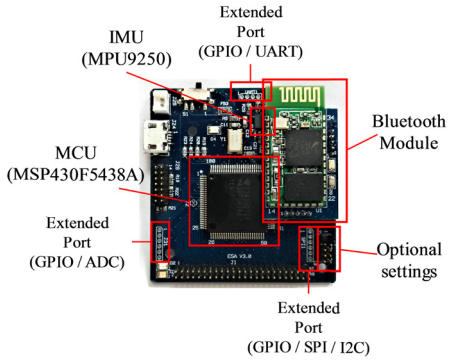

Fig. 3. Photograph of the mainboard.

and three-axis Euler angles of each finger segment are obtained using the sensor fusion algorithm.

The sensorized glove comprises three parts: mainboard, IMU glove module, and five FSRs. The total mass of the proposed device is 70 g. The prototype of the sensorized glove is displayed in Fig. 2.

A. Mainboard

Fig. 3 displays a photograph of the mainboard with a size of 43 × 45 × 1 mm^3. The mainboard is the core of the entire system and is mounted on the subject's forearm by using Velcro. A 3.7-V Li-ion polymer battery with 1000 mAh capacity provides power to the entire system and can last for 5 h. The microcontroller unit (MCU) (MSP430F5438A, Texas Instruments, Dallas, TX, USA) mounted on the mainboard was used to communicate with all the other components on the

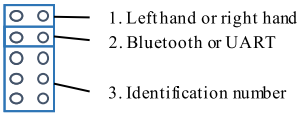

Fig. 4. Definition and purpose of the optional setting jumper connector.

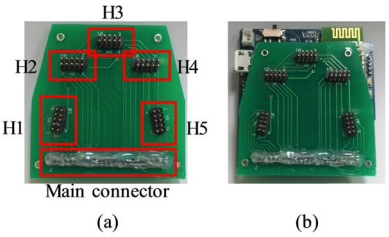

Fig. 5. Photographs of the adapter board. (a) Front side photograph displays the position of each connector; (b) Combination of the adapter board and main board.

sensorized glove. The MCU collects data from IMUs via a SPI bus and encapsulates the data into packets. The packets are sent to the evaluation program via Bluetooth or UART at a frequency of 50 Hz.

To enhance the extensibility of the mainboard, three extended ports were used that together provide interfaces of SPI, I2C, UART, ADC, and GPIO for extending the system in future. Moreover, to increase the flexibility of the system, a 10-pin jumper connector was used to provide three optional settings for users, as shown in Fig. 3. The definition and purpose of each setting are presented in Fig. 4. In setting 1, if the two pins are connected, it implies that the right hand mode is selected. Otherwise, it implies that the left hand mode is selected. In setting 2, when the two pins are connected, the UART mode is selected. Otherwise, the Bluetooth mode is selected. In setting 3, a switch is provided between the glove and the mainboard modes. In the glove mode, 18 IMUs are adopted to record hand movements. In the mainboard mode, only the IMU on the mainboard is adopted. The three pairs of pins can provide eight different identification numbers. If the identification number is zero, then the glove mode is selected. Otherwise, the mainboard mode is selected, and the identification number is the mainboard's identifier. By using this protocol, the mainboard in the glove mode can be combined with the other mainboards in the mainboard mode to construct an upper-limb motion tracking system.

B. IMU Glove Module

The IMU glove module mainly comprises two parts: the adapter board and the five IMU flexible boards. The adapter board processes the data from the IMUs on the IMU flexible boards. Fig. 5 (a) presents the position of each connector on the adapter board. The adapter board contains five connectors for connecting the IMU flexible boards—H1 to H5—and one main connector for combining and communicating with the main board. The adapter board was designed as a hexagon for easily combining it with the mainboard displayed in Fig. 5 (b). The positions of H1 and H5 are different from the other three connectors because H1 and H5 mainly record the data from

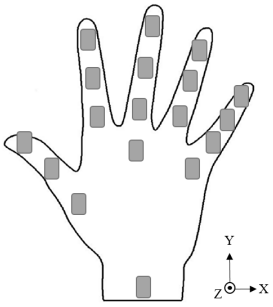

Fig. 6. Position and axes of each IMU.

the thumb and little finger, which have higher degrees of freedom and higher flexibility than the other fingers. When the right hand mode is selected, the sequence from the thumb to little fingers is from H1 to H5. Conversely, when the left hand mode is selected, the sequence from thumb to the little finger is from H5 to H1. This flexible design let users wear the same sensorized glove on both left and right hands by modifying the suitable length of the flexible boards and setting the right or left hand mode. To enhance safety, all of the back sides of the connectors were insulated with a hot melt adhesive.

17 IMUs are on the five IMU flexible boards and one IMU is on the forearm. The positions of the 18 IMUs on the sensorized glove are presented in Fig. 6. Each IMU consists of a three-axis accelerometer, a three-axis gyroscope, and a three-axis magnetometer, which provides three-axis acceleration, three-axis angular rate, and three-axis magnetic field. The resolutions of the sensors were set as follows: ± 16 g for the accelerometer, ± 2000 dps for the gyroscope, and ± 4800 μT for the magnetometer. The IMU flexible boards for the middle and little fingers contain four IMUs. The IMU flexible boards for the thumb, index, and ring fingers contain three IMUs. The reason of this design was the inspiration from the study by Kortier *et al*[6]. The study by Kortier included three IMUs. The first IMU belonged to the thumb, the second IMU was for the middle finger, and the last IMU was for the little finger. These IMUs were attached on the back of hand to obtain higher joint angle estimation accuracy for the MCP joint because the hand can flex horizontally and forward. Therefore, in the present study, these three IMU sensors were attached on the back of hand to calculate the angle of the MCP joint.

Here, 17 IMUs were soldered on flexible PCBs to form five IMU flexible boards. Each IMU flexible board is 20.5 cm long and can contain up to four IMUs. The prototype of the IMU flexible board is displayed in Fig. 7. A connector was used on the IMU flexible board for communicating with the adapter board. By using the flat flexible cable, the IMU flexible board could be easily mounted on the adapter board. To protect the IMUs on the flexible PCB, a special material known as FR-4 was attached on the back of each IMU to enhance the durability of the flexible PCBs. Moreover, to stably pull and plug on the adapter board, the connector on the IMU flexible board was protected with a hot melt adhesive. To enhance the mobility of the device and ensure that the device fits hands of various sizes when wearing the glove, a customized Velcro

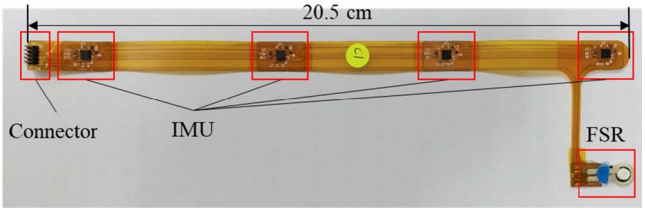

Fig. 7. Prototype of the IMU flexible board.

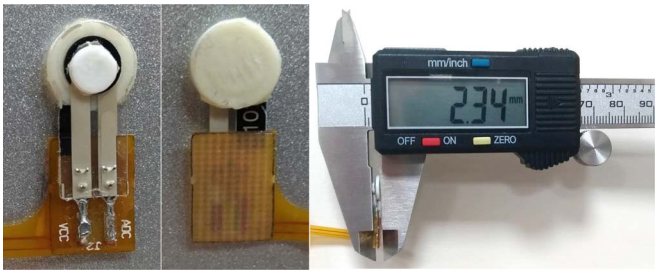

Fig. 8. Rigid disks for enhancing the repeatability of the FSR: (a) disk on the front side, (b) disk on the back side, and (c) the side view of the force sensing area.

string was used and attached to the IMU sensing area on the top side of the finger segment.

C. FSR

To measure the finger force, FSRs can be optionally soldered on the force sensing pad of the IMU flexible boards. A light FSR with high linearity and reliability (FlexiForce A101, Tekscan, Boston, MA, USA) was adopted in this study [20]. The resistance of the FSR varies with the force applied on the sensing area. Based on the FSR datasheet, the conductance of FSR and force has a highly linear relation. However, the surface of fingertip is uneven and would unevenly pressure on the FSR. Such a pressure may cause nonlinearity between the conductance of FSR and force [21]. To enhance the linearity and repeatability of the FSRs, it is necessary to attach two rigid disks on the top and bottom of the FSR [22]. In this study, two polymer disks constructed using a reliable 3D printer (da Vinci 1.0, XYZprinting, New Taipei City, Taiwan) were used, as displayed in Fig. 8. The diameters of the two disks are 7.6 and 3.8 mm for the back and front side, respectively, and the thickness of the two disks is 1 mm. The total thickness of the force sensing area is 2.34 mm. To stably attach the FSR on the surface of a fingertip, a finger cot cut from a clinical glove was used. The advantage of using a clinical glove as the material for the finger cot is that it can perfectly fit various sizes of fingertips of different users. Thus, this avoids the FSRs from slipping out of the fingertip.

A DC voltage divider circuit with a 10 KΩ resistor and FSR was used to obtain the conductance relation of FSR and force. For verification, a reliable digital force gauge (DS-50, DESIK, Germany) was adopted to apply stable force to the FSRs and then obtain the relative divided voltage output. The stable force was set from 4.9 to 44 N because the FSRs can measure the force up to 44 N. The interval between every two forces was set to 4.9 N to obtain a more accurate linear relation

between the conductance of FSR and force. Conditioning of the FSRs was required to ensure the repeatability of FSR before measuring the force. The measurement was conducted five times for each FSR to obtain a more reliable result. After conducting five measurements, the average of the divided voltages of the five measurements corresponding to each force setting was obtained. Because the output of the FSR is voltage, a formula to convert the output voltage into the relative conductance is required. The converting formula is expressed in (1):

$$C = \frac{V}{10000 \times (3.3 - \mathrm{V})}, \tag{1}$$

where C is the relative conductance of the FSR, and V is the output voltage of the voltage divider. After obtaining the conductance of each FSR, a two-degree polynomial regression was applied to obtain the parameters of the function that converts the conductance of FSR to force. The formula is expressed in (2)

$$F = a_2 C^2 + a_1 C + a_0, \tag{2}$$

where $F$is the force predicted by the formula, and a_0 to a_2 are the parameters obtained from the polynomial regression. However, because the characteristic of each FSR differs widely, a_0 to a_2 would be different for each FSR sensor.

III. Algorithms

After receiving the IMU sensor packet, the C# program in the host processes the packet. The algorithm in the program estimates the Euler angles of each sensor and joint angle of every two adjacent finger segments. Moreover, the force was also estimated by applying the formula expressed in (2).

A. Magnetometer Calibration and Sensor Fusion Algorithm

Fig. 9 presents the calibration process and the fusion algorithm application process. After receiving the data packet, the program immediately parses the data packet into the values of acceleration, angular rate, magnetic field, and the divided voltage of FSR. To obtain more reliable data, the calibration of each sensor is necessary. As the acceleration and angular rate values are calibrated automatically when the sensorized glove is switched on, only the magnetometer calibration is conducted in the program. After the magnetometer calibration, the calibrated data of acceleration, angular rate, and magnetic field are processed using the sensor fusion algorithm to obtain the attitude quaternion at the current time. After obtaining the quaternion, the Euler angle of each IMU sensor and the joint angle between every two adjacent IMU sensors can be calculated. Moreover, the fingertip force is simultaneously estimated from the divided voltage of the FSR.

The magnetometer calibration is the most crucial step before sensor fusion because the magnetometers in the IMUs are easily affected by the magnetic field disturbances in the environment. To reduce the complexity of computation, an easy and efficient approach was adopted [23]. When the connection between the sensorized glove and the program in the host is established, the first 2000 samples from each axis of the

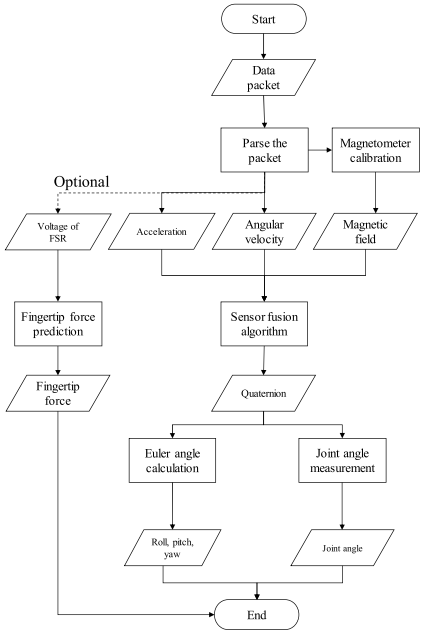

Fig. 9. Process of calibration and fusion algorithm application.

magnetometer are collected for calibration. The calibration includes hard-iron and soft-iron calibrations. The aim of hard-iron calibration is to eliminate the hard-iron distortion due to the materials that exhibit a constant magnetic field due to the earth's magnetic field. The aim of soft-iron calibration is to eliminate the soft-iron distortion due to the material distortion due to the magnetic field. The calibration vector for hard-iron calibration is expressed in (3). δ_x, δ_y, and δ_z denote the x-, y-, and z-axis offsets of the magnetic fields, respectively. S_x, S_y, and S_z denote the 2000 magnetic field data series obtained for calibration from the x, y, and z axes, respectively. δ_x, δ_y, and δ_z are obtained by averaging the maximum and minimum values of S_x, S_y, and S_z. The calibrating vectors for soft-iron calibration are expressed in (4) and (5). To conduct the soft-iron calibration, the scale bias for each axis is required. γ_x, γ_y, and γ_z are the max chord lengths of each axis. ϵ_x, ϵ_y, and ϵ_z are the scale biases for each axis. Therefore, the formula for obtaining the calibrated magnetic field data is expressed in (6). m_x, m_y, and m_z represent the original data of the magnetic field. m'_x, m'_y, and m'_z denote the calibrated data. After the magnetometer calibration, the magnetic data becomes reliable, and the sensor fusion algorithm can be applied to obtain the current attitude.

$$\begin{bmatrix} \delta_x \\ \delta_y \\ \delta_z \end{bmatrix} = \frac{1}{2} \cdot \begin{bmatrix} maxS_x + minS_x \\ maxS_y + minS_y \\ maxS_z + minS_z \end{bmatrix} \tag{3}$$

$$\begin{bmatrix} \gamma_x \\ \gamma_y \\ \gamma_z \end{bmatrix} = \frac{1}{2} \cdot \begin{bmatrix} maxS_x - minS_x \\ maxS_y - minS_y \\ maxS_z - minS_z \end{bmatrix} \tag{4}$$

$$\begin{bmatrix} \epsilon_x \\ \epsilon_y \\ \epsilon_z \end{bmatrix} = \frac{3}{\gamma_x + \gamma_y + \gamma_z} \cdot \begin{bmatrix} \gamma_x \\ \gamma_y \\ \gamma_z \end{bmatrix} \tag{5}$$

$$\begin{bmatrix} m'_x \\ m'_y \\ m'_z \end{bmatrix} = \begin{bmatrix} \epsilon_x(m_x - \delta_x) \\ \epsilon_y(m_y - \delta_y) \\ \epsilon_z(m_z - \delta_z) \end{bmatrix} \tag{6}$$

In this study, an efficient sensor fusion algorithm proposed by Madgwick [24] was adopted. The gradient descent approach was applied to obtain an optimal result in each updating process. The optimal result of attitude can be defined as a quaternion, as expressed in (7). Here, q_t represents the attitude at the current time, q_{t-1} is the attitude at the previous time, ω_{t-1} is the angular rate at the previous time, σ_{t-1} is the time difference between the previous and current time, and β is the error of the gyroscope. In this study, β was set at 0.6 based to obtain the optimal result. $\frac{\nabla f}{\|\nabla f\|}$ is the gradient defined on the basis of the measurement from the accelerometer and magnetometer.

$$q_t = q_{t-1} + \frac{q_{t-1} \times \omega_{t-1}\sigma_{t-1}}{2} - \beta \frac{\nabla f}{\|\nabla f\|}\sigma_{t-1} \tag{7}$$

Every rotation can be defined as the attitude on the x, y, and z axes. After obtaining the quaternion of the current attitude from (7), the quaternion can be converted into a Euler angle in the Z–Y–X sequence [25]. The conversion is presented in (8). q_0, q_1, q_2, and q_3 are the components of q_t. φ represents the roll value, which is the attitude on the x axis. θ is the pitch value, which implies the attitude on the y axis. ψ denotes the yaw value, which implies the attitude on the $z$axis. After converting the quaternion to a Euler angle representation, the 3D attitude for each sensor is obtained. The 3D attitude can be used as additional information to represent a hand's 3D movement.

$$\begin{bmatrix} \varphi \\ \theta \\ \psi \end{bmatrix} = \begin{bmatrix} \text{atan2}\dfrac{2\left(q_0q_1 + q_2q_3\right)}{1 - 2\left(q_1^2 + q_2^2\right)} \\ \text{asin}(2(q_0q_2 - q_3q_1)) \\ \text{atan2}\dfrac{2\left(q_0q_3 + q_1q_2\right)}{1 - 2\left(q_2^2 + q_3^2\right)} \end{bmatrix} \tag{8}$$

B. Joint Angle Estimation

For physicians, the assessment of joint angles of every two adjacent finger segments is a primary criterion to evaluate the progress of rehabilitation [13]. The program in the host calculates not only the Euler angle for 3D rotations but also joint angles for enabling the physicians. To determine the real attitude of two adjacent IMUs, two vectors, v_1 and v_2, were equally initialized to (0, 0, 1). After initialization, the current attitude quaternions of the two adjacent IMUs that are defined as q_1 and q_2 are applied on v_1 and v_2, respectively. The formula of applying the rotation (q_0, q_1, q_2, q_3) on the initialized vector (v_x, v_y, v_z) is presented in (9). The vector after rotation is (v'_x, v'_y, v'_z). After obtaining the two adjacent vectors, the flexion angle θ_r between v'_1 and v'_2 can be calculated in (10).

$$\begin{bmatrix} v'_x \\ v'_y \\ v'_z \end{bmatrix} = \begin{bmatrix} 1 - 2q_2^2 - 2q_3^2 & 2(q_1q_2 + q_0q_3) & 2(q_1q_3 - q_0q_2) \\ 2(q_1q_2 - q_0q_3) & 1 - 2q_1^2 - 2q_3^2 & 2(q_2q_3 + q_0q_1) \\ 2(q_1q_3 + q_0q_2) & 2(q_2q_3 - q_0q_1) & 1 - 2q_1^2 - 2q_2^2 \end{bmatrix} \times \begin{bmatrix} v_x \\ v_y \\ v_z \end{bmatrix} \tag{9}$$

$$\theta_r = \frac{180}{\pi} \cos^{-1}\left(\frac{v'_1 \cdot v'_2}{\|v'_1\| \|v'_2\|}\right) \tag{10}$$

Fig. 10. Positions of seven markers for measuring the actual PIP and DIP.

IV. Verification of the Sensorized Glove

To ensure the reliability of a sensorized glove, the verification of a sensorized glove includes the verification of joint angles and that of FSR. Subsequently, the comprehensive verification of the combination of joint angle and fingertip force was also conducted to ensure that the sensorized glove can simultaneously measure the joint angles and fingertip force.

A. Verification of Joint Angle Estimation

The purpose of verifying joint angle is to ensure that the joint angle calculated by the algorithm is reliable and accurate for hand function assessment. A participant was asked to wear the glove and perform the experimental tasks, and the program in the host was programmed to simultaneously calculate and record the joint angle. A reliable optical motion capturing system (Vicon Nexus 1.7.1, Vicon, Oxford, UK) was used as a ground truth for comparison with the motion estimation from a sensorized glove. Before the participant began performing the experiment, seven markers for capturing the participant's finger motion were pasted on the both sides of finger's root, proximal interphalangeal (PIP), distal interphalangeal (DIP), and fingertip. The diameter of the marker is 7 mm. The positions of the seven markers are displayed in Fig. 10. To obtain reliable and stable experimental results, a customized tool for repetitive grasping was adopted in the experiment. The repetitive grasping movements include two parts: vertical flexion–extension and horizontal flexion–extension tasks. The purpose of separating the vertical and horizontal tasks is that none of the related studies verified joint angle variation in the horizontal flexion–extension situation. However, the horizontal flexion–extension movement is an important criterion for certain tasks for hand function assessment. The tasks conducted by involving vertical flexion–extension and horizontal flexion–extension movements are respectively displayed in Fig. 11 (a) and Fig. 11 (b) . To simplify the verification process by using a Vicon motion capturing system, only one IMU flexible board was used on the participant's index finger. The reasons for selecting the index finger are to avoid the occlusion of the Vicon motion capturing system and collision of markers and due to the index finger being one of the most important fingers for conducting daily activities [1]. For both vertical and horizontal flexion–extension movements, the participant was asked to perform full extension and full flexion five times. Each full extension or full flexion lasts for 3 s. Therefore, approximately 30 s are required for each task. Furthermore,

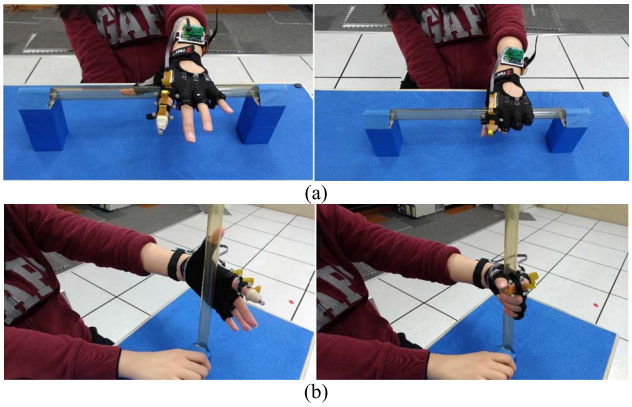

Fig. 11. Repetitive tasks to evaluate the reliability of the proposed sensorized glove: (a) vertical flexion–extension movement, and (b) horizontal flexion–extension movement.

Fig. 12. Applying force on the force gauge.

to evaluate the practical situation when using the sensorized glove, the participant was asked to continuously perform random fast-paced and slow-paced flexion–extension movements in a 3D situation for 10 s. The purpose of the random movement experiment was to verify that the sensorized glove has the ability to accurately capture the hand motion in any possible clinical situation. After conducting the verification, a comparison between the result of the Vicon motion capturing system and that of the sensorized glove was conducted.

B. Verification of FSR

The purpose of verifying FSR is to ensure that the fingertip force estimated from the FSR is accurate and reliable. To simplify the verification of the converting formula, only one FSR was used in this experiment. To obtain the ground truth of the fingertip force, the measuring function in the force gauge was used. The participant was asked to wear the sensorized glove and press on the sensing area of the force gauge. When the participant's fingertip was applying force on the force gauge, the force gauge simultaneously recorded the measured force and transmitted the measured value to the host via UART. Moreover, the developed program in the host received the FSR data from the sensorized glove and then calculated the fingertip force. The process of applying force on the force gauge is presented in Fig. 12. After conducting the verification, a comparison between the force from the force gauge and the force from the FSR on the sensorized glove was conducted.

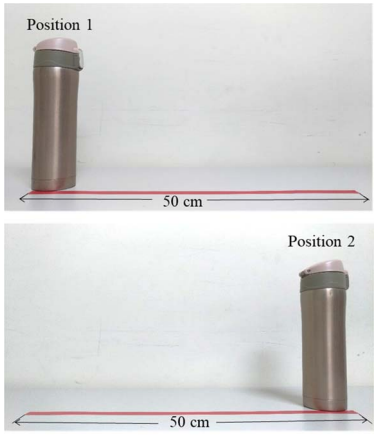

Fig. 13. Comprehensive evaluation of both joint angle and fingertip force estimation.

C. Comprehensive Evaluation of Joint Angle and Fingertip Force

One of the primary contributions of this study is to provide the joint angle and fingertip force of each finger simultaneously when the user is conducting the tasks for assessing the hand function. Therefore, the comprehensive evaluation of both joint angle and fingertip force estimation is necessary. A subject with a mild hand movement disorder and a healthy subject were recruited to conduct the same hand function assessment tasks. The task of moving a bottle filled with water was used to evaluate the difference between the subject with a mild hand movement disorder and the healthy subject. The process of the experiment is presented in Fig. 13. The two participants were asked to hold and lift up the bottle from position 1 and move it to position 2. The distance between these two positions is 50 cm. The joint angle and fingertip force of each finger can be recorded. The values obtained for the subject with a mild hand movement disorder and the healthy subject were compared. All procedures and measurements in this study were performed in accordance with the World Medical Association, Declaration of Helsinki – Ethical Principles for Medical Research Involving Human Subjects (version October 2013).

V. Results

A. Verification Results of Joint Angle Estimation

The mean absolute error (MAE) was calculated to evaluate the accuracy of estimating the joint angle by using the proposed sensorized glove. As markers of the Vicon motion capturing system and the IMUs were attached on different positions of the fingers, the joint angles at the initial posture in each task, namely the initial reference, were obtained from the average of the first 100 recordings of joint angles from the two systems. Subsequently, the initial references were subtracted from the joint angles in the following measurements from the two systems to make the comparison more reliable.

Table I presents the MAE between the joint angles provided by the sensorized glove and that provided by the motion capturing system when the subject was conducting repetitive

TABLE I
MAE OF REPETITIVE TASKS

Task	PIP (°)	DIP (°)	Average (°)
Vertical Flexion-Extension	2.62	4.76	3.69
Horizontal Flexion-Extension	2.39	4.53	3.46

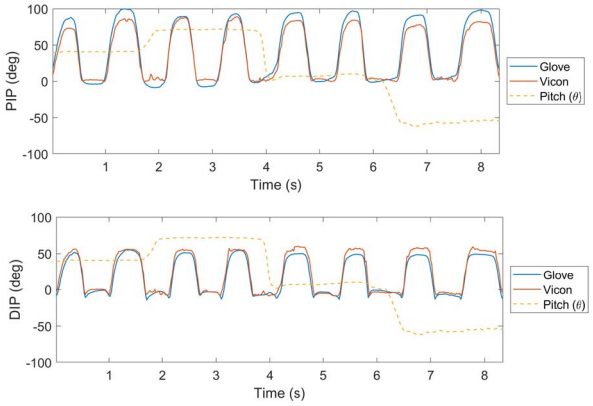

Fig. 14. Random flexion–extension tasks at low speed.

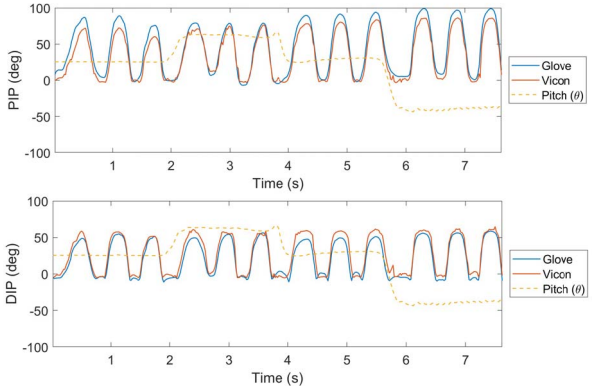

Fig. 15. Random flexion–extension tasks at high speed.

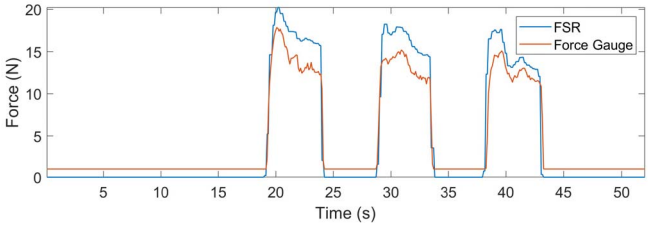

Fig. 16. Comparison between the actual force and predicted force.

flexion–extension tasks. For vertical flexion–extension tasks, the MAE of PIP and DIP are 2.62° and 4.76°, respectively, and the average MAE is 3.69°. For horizontal flexion–extension tasks, the MAE of PIP and DIP are 2.39° and 4.53°, respectively, and the average MAE is 3.46°.

Fig. 14 displays an example of the joint angles of PIP and DIP when the participant's index finger was performing random flexion–extension tasks at low speed. The pitch angle θ provided by the sensorized glove was adopted to record pronation and supination of the wrist and to prove that the joint angle estimation can be conducted when the participant's wrist is pronating or supinating. The variation in θ is represented by a yellow dotted line in Fig. 14. The blue line is a joint angle provided by the sensorized glove, and the orange line is the joint angle provided by the Vicon motion capturing system. The MAE of PIP and DIP is 6.09° and 2.81°, respectively. The average MAE is 4.45°when performing random flexion–extension tasks at low speed.

Fig. 15 displays an example of the joint angles of PIP and DIP when the participant's index finger performed random flexion–extension tasks at high speed. The MAE of PIP and DIP was 4.32° and 4.40°, respectively. The average MAE was 4.36° when performing random flexion–extension tasks at high speed.

B. Verification Results of FSR

Fig. 16 presents a comparison between the actual force and predicted force. The blue line represents the force predicted by the FSR on the sensorized glove, and the orange line denotes the actual force provided by the force gauge. The MAE between the two results is 1.47 N.

C. Comprehensive Evaluation of the Joint Angle and Fingertip Force

Fig. 17 reveals that the proposed sensorized glove can simultaneously capture a finger's joint angles and fingertip forces when the healthy subject and the subject with a mild hand movement disorder perform the task of moving the bottle. The comparison between the healthy subject and the subject with a mild hand movement disorder was also conducted. To simplify the comparison, only the result of three fingers, that is, the thumb, index finger, and little finger, are demonstrated in Fig. 17. Fig. 17 (a) and Fig. 17 (b) depict the variation in the joint angles and fingertip forces of the healthy subject and the subject with a mild hand movement disorder, respectively. The result reveals that the variation in the healthy subject's joint angles is more stable than that in the joint angles of the subject with a mild hand movement disorder. Moreover, the fingertip force of the healthy subject's thumb is higher than the thumb force of the subject with a mild hand movement disorder, thus revealing that the healthy subject owns a stronger fingertip force.

Although Fig. 17 proves that the sensorized glove can record a finger's movement and fingertip force simultaneously, some slight characteristics of a finger's movement are still difficult to recognize. To solve this problem, the sensorized glove provided the acceleration and angular rate of each IMU. For example, Fig. 18 presents the three-axis accelerations from the IMU on index finger's tip when the subjects were performing the entire bottle moving task. The red frame in Fig. 18 indicates the signals displayed in Fig. 17. The result reveals that the finger movement of the subject with a mild hand movement disorder contains a higher amount of jitter than the finger movement of the healthy subject. This result indicates that the fingers of the subject with mild hand movement disorder were trembling when resting and moving the bottle.

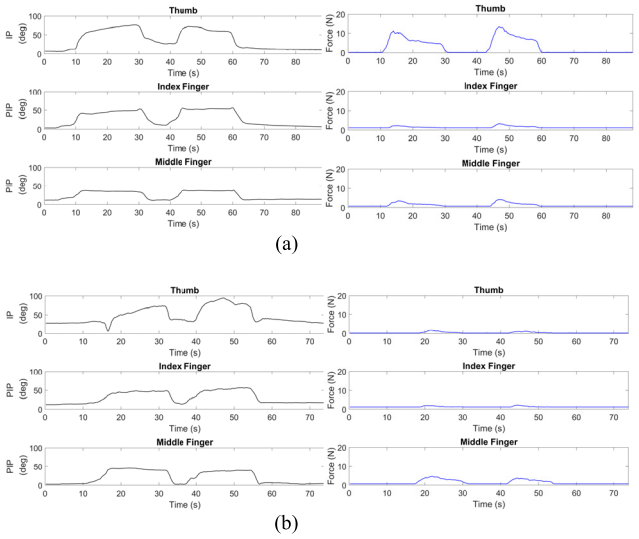

Fig. 17. Result of the comprehensive evaluation of the joint angle and fingertip force: (a) left side: joint angles of the healthy subject's fingers; right side: fingertip forces of the healthy subject's fingers and (b) left side: joint angles of the fingers of the subject with a mild hand movement disorder; right side: fingertip forces of the fingers of the subject with a mild hand movement disorder.

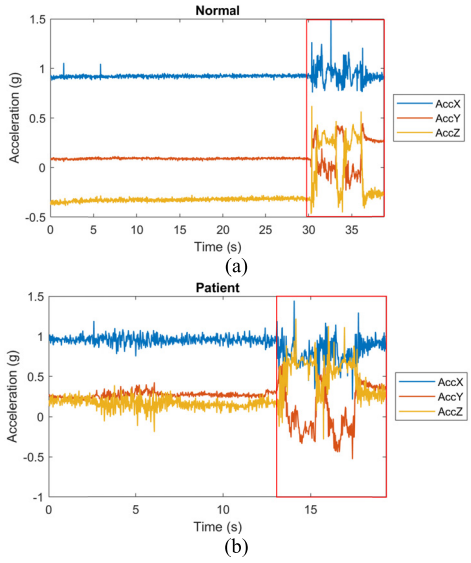

Fig. 18. Acceleration of the IMU on the tip of index finger: (a) healthy subject and (b) subject with a mild hand movement disorder.

VI. Discussion

This study proposed a sensorized glove that can automatically capture the finger motion and fingertip force when a subject is conducting hand function assessment dynamically. To evaluate the accuracy and reliability of the proposed sensorized glove, three verifications were conducted. First, the accuracy of measuring the joint angle was verified by calculating the MAE between the joint angles provided by the sensorized glove and that provided by the Vicon motion capturing system. Four experiments including vertical flexion–extension, horizontal flexion–extension, random flexion–extension tasks at low speed and random flexion–extension tasks at high speed were conducted. Table I indicates that the MAEs of the repetitive flexion–extension tasks are all between 2° and 5°. The error might be caused by the position where the IMUs were attached. Moreover, the offsets obtained from the magnetometer calibration slightly affected the IMU's attitude and further affected the joint angle estimation. As shown in Figs. 14 and 15, for random flexion–extension tasks, the average MAE at low and high speeds are 4.45° and 4.36°, respectively. Both of the results are <5°. The errors are mainly due to two potential reasons. One reason is that the markers of the Vicon motion capturing system were mainly placed on both sides of the finger joints. This position can cause instability or be occluded when the subjects perform 3D flexion–extension tasks. Therefore, as presented in Figs. 14 and 15, the joint angles obtained from the Vicon motion capturing system have more jitters than the joint angles estimated using the data glove. According to the related research, the accuracy of the manual goniometer is 4–5° [26]. Although the errors exist, the accuracy is still acceptable for physicians to measure hand kinematics and assess the hand function during patients' rehabilitation. Second, the verification of the fingertip force estimated by using the FSR was also conducted. The result presented in Fig. 16 shows that the MAE between the actual force and the force estimated by FSR is 1.47 N. The error was mainly caused by the characteristics of FSR. Although the FSRs used on this sensorized glove have a relatively high linearity, a bias still exists and varies based on different conditioning statuses [20]. However, the accuracy of the FSR is still sufficiently robust to assess the subjects' fingertip force [27]. Third, to verify if the sensorized glove is practical and reliable in a practical rehabilitation setting, a comprehensive evaluation of joint angles and fingertip force estimation was conducted. The healthy subject and the subject with a mild hand movement disorder were asked to perform the bottle moving task, which is a common activity in the daily life. Fig. 17 presents the differences between the joint angles and fingertip forces of the healthy subject and the subject with a mild hand movement disorder when the two subjects were performing the same task. For the subject with a mild hand movement disorder, the change in joint angles is slightly unstable, particularly for the thumb and index finger, which are the most important fingers when performing the task. Moreover, the thumb tip force of the subject with a mild hand movement disorder is quite smaller than the force of the healthy subject. The result indicates that although the subject with a mild hand movement disorder could lift up and move the bottle completely, he was still struggling with the moving task and could not perform the task stably and smoothly. To present additional evidence for this assumption, the acceleration of the IMU on index finger's tip was recorded, as presented in Fig. 18, indicating that the healthy subject's finger is stable, whereas the finger of the subject with a mild hand movement disorder is trembling on three axes whenever resting or moving the bottle. The conventional assessment of these disorders is mainly performed by physicians or therapists by measuring the finger joint angles with goniometers and fingertip force with force gauges. However, the conventional methods can only be used for measuring the hand movements in static tasks. The proposed sensorized glove measures the hand kinematics and fingertip force automatically while the subject conducts

TABLE II
COMPARISON BETWEEN THE PROPOSED SENSORIZED GLOVE AND OTHER SYSTEMS

System	Kortier *et al.* [6]	Lin *et al.* [14]	Salchow-Hömmen *et al.* [15]	Liu *et al.* [19]	Our proposed sensorized glove
Extensibility	No	Yes	No	No	Yes
Left/right hand swap	No	No	No	No	Yes
Provided information	Joint angles, positions	Raw data, Euler angles	Positions	Joint angles	Raw data, Euler angles, joint angles
Fingertip force	No	No	No	Yes	Yes
Verification of fingertip force	N/A	N/A	N/A	No	Yes
Verification platform	Hand	Robotic platform	Hand	Rigid bends (Static)	Hand
Verifications of random 3D movements	No	No	No	No	Yes

the dynamic hand movements. The sensorized glove also combines the measurements of fingers' joint angles, fingertip forces, and raw data from each IMU to comprehensively assess the subjects' hand function.

The proposed sensorized glove and the methods proposed in other related studies are compared in Table II . To focus on the most related studies, the proposed sensorized glove is only compared with the sensorized gloves with a modular design and the sensorized gloves equipped with force sensors. In terms of extensibility, only our proposed sensorized glove provides extended ports for combining it with other biomedical sensors. To enhance the flexibility and practicality of the system, only the proposed sensorized glove is equipped with the Bluetooth/UART, left–right hand, and identification number settings. Therefore, the proposed sensorized glove is more flexible than other sensorized gloves listed in Table II . For comparing the information provided by the glove, Kortier *et al.* and Salchow-Hömmen *et al.* mainly focused on the position of each IMUs, whereas Lin *et al.*and the proposed sensorized glove focused on the relation between two adjacent IMUs, such as joint angles. All of the related studies provided the required information to track hand motion in various aspects. Nonetheless, only the proposed sensorized glove and the glove proposed by Liu *et al.*provide the fingertip force, which is a necessary criterion for hand function evaluation. Although the glove proposed by Liu *et al.*adopted more force sensors to measure the force of fingers and the palm, the accuracy and reliability of those sensors was not validated. For validating the reliability and accuracy of the kinematic measurement, only Lin *et al.* and Liu*et al.*used a robotic platform or rigid bends. However, other studies conducted the verification by wearing the glove, which is more similar to the practical clinical situation. In all of the compared studies, only our proposed system conducted the verification of 3D flexion–extension tasks with random wrist pronation and supination. This is necessary for simulating the practical rehabilitation setting. By analyzing Table II , it can be concluded that most of the considered studies have substantial benefits, but some limitations are still required to be addressed. Our proposed sensorized glove exhibits the advantages of the previous studies and can be expanded to comprehensively track hand kinematics and fingertip force. However, there are still some limitations that should be solved in the future. The first limitation is that the proposed sensorized glove currently focuses on joint angle measurement and fingertip force estimation but cannot obtain the displacement and moving trajectory of each sensor. Therefore, the algorithm of estimating displacement and moving trajectory will be involved in the next version of the sensorized glove. The second limitation is that magnetometers can be affected by the environment if the magnetometer is not well calibrated. To solve this problem, ferromagnetic materials should be removed to ensure that the environmental magnetic field is stable when using this sensorized glove. Moreover, a more robust magnetometer calibration algorithm should be developed and applied in a further study.

VII. CONCLUSION

This study proposed a sensorized glove combining nine-axis IMUs and FSRs to provide not only kinematic data including raw data of each IMU, Euler angles, and joint angles of each joint but also force data including fingertip force. Three verifications were conducted to verify the sensorized glove's accuracy and reliability. The verification results reveal a high accuracy for estimating the joint angles and fingertip force. Furthermore, a comprehensive estimation of joint angles and fingertip force reveals that the system can record joint angle and fingertip force simultaneously. The difference between a healthy subject and a subject with mild hand movement disorder can be observed from the data recorded when performing the task of moving a bottle. In summary, there are three main contributions of the proposed sensorized glove. First, the sensorized glove is combined with FSRs to provide fingertip force, which is a critical criterion during hand function assessment. Second, the probability of extensibility of the sensorized glove is high. The sensorized glove has a modular design and provides an extended port for combining with other biomedical sensors. A 10-pin jumper connector was designed to enhance the flexibility of the system for enabling user optional settings. Third, only the proposed sensorized glove conducted 3D flexion–extension tasks with pronating and supinating the wrist, and this test reveals an acceptable accuracy. The evidence and contributions indicate that the proposed sensorized glove has a strong potential application in the practical rehabilitation field. In the future, attempts will be made to solve two problems including moving trajectory [28] and magnetometer calibration, and more participants will be recruited to the clinical experiments for hand function assessment. In addition to the accuracy of measuring the hand kinematics, the repeatability is also important and should also be verified before conducting large-scale clinical experiments to ensure the sensorized glove will have the same outcome in

thousands of repetitive experimental setting. Moreover, data analysis and machine learning techniques will also be included in the future studies to construct a robust and efficient system for automated hand function assessment.

REFERENCES

[1] W. Muellbacher, C. Richards, and U. Ziemann, "Improving hand function in chronic stroke," *Arch. Neurol.*, vol. 59, no. 8, pp. 1278–1282, 2002.

[2] F. D. Kutz, A. Wölfel, T. Meindl, D. Timmann, and P. F. Kolb, "Spatio-temporal human grip force analysis via sensor arrays," *Sensors*, vol. 9, no. 8, pp. 6330–6345, 2009.

[3] J. G. Young, M. E. Sackllah, and T. J. Armstrong, "Force distribution at the hand/handle interface for grip and pull tasks," in *Proc. Hum. Factors Ergon. Soc. Annu. Meet.*, 2010, vol. 54, no. 15, pp. 1159–1163.

[4] M. Térémetz *et al.*, "A novel method for the quantification of key components of manual dexterity after stroke," *J. Neuroeng. Rehabil.*, vol. 12, no. 64, pp. 1–16, 2015.

[5] N. Carbonaro, G. D. Mura, F. Lorussi, R. Paradiso, D. De Rossi, and A. Tognetti, "Exploiting wearable goniometer technology for motion sensing gloves," *IEEE J. Biomed. Health Inform.*, vol. 18, no. 6, pp. 1788–1795, Nov. 2014.

[6] H. G. Kortier, V. I. Sluiter, D. Roetenberg, and P. H. Veltink, "Assessment of hand kinematics using inertial and magnetic sensors," *J. Neuroeng. Rehabil.*, vol. 11, no. 70, pp. 1–15, 2014.

[7] A. Erol, G. Bebis, M. Nicolescu, R. D. Boyle, and X. Twombly, "Vision-based hand pose estimation: A review," *Comput. Vis. Image Understand.*, vol. 108, nos. 1–2, pp. 52–73, Oct./Nov. 2007.

[8] V. Venkataraman *et al.*, "Component-level tuning of kinematic features from composite therapist impressions of movement quality," *IEEE J. Biomed. Health Informat.*, vol. 20, no. 1, pp. 143–152, Jan. 2016.

[9] X. Li, R. Wen, Z. Shen, Z. Wang, K. D. K. Luk, and Y. Hu, "A wearable detector for simultaneous finger joint motion measurement," *IEEE Trans. Biomed. Circuits Syst.*, vol. 12, no. 3, pp. 644–654, Jun. 2018.

[10] A. Leoni *et al.*, "A 10-17 DOF sensory gloves with harvesting capability for smart healthcare," *J. Commun. Softw. Syst.*, vol. 15, no. 2, pp. 1–7, 2019.

[11] Y. Choi, K. Yoo, S. J. Kang, B. Seo, and S. K. Kim, "Development of a low-cost wearable sensing glove with multiple inertial sensors and a light and fast orientation estimation algorithm," *J. Supercomput.*, vol. 74, no. 8, pp. 3639–3652, 2018.

[12] B. Fang, F. Sun, H. Liu, and D. Guo, "Development of a wearable device for motion capturing based on magnetic and inertial measurement units," *Sci. Program.*, vol. 2017, pp. 1–11, 2017, Art. no. 7594763.

[13] J. Connolly, J. Condell, B. O'Flynn, J. T. Sanchez, and P. Gardiner, "IMU sensor-based electronic goniometric glove for clinical finger movement analysis," *IEEE Sensors J.*, vol. 18, no. 3, pp. 1273–1281, Feb. 1, 2018.

[14] B.-S. Lin, I.-J. Lee, S.-Y. Yang, Y.-C. Lo, J. Lee, and J.-L. Chen, "Design of an inertial-sensor-based data glove for hand function evaluation," *Sensors*, vol. 18, no. 5, article 1545, pp. 1–17, Feb. 1, 2018.

[15] C. Salchow-Hömmen, L. Callies, D. Laidig, M. Valtin, T. Schauer, and T. Seel, "A tangible solution for hand motion tracking in clinical applications," *Sensors*, vol. 19, no. 1, p. 208, 2019.

[16] A. Rashid and O. Hasan, "Wearable technologies for hand joints monitoring for rehabilitation: A survey," *Microelectron. J.*, vol. 88, pp. 173–183, Jun. 2019.

[17] P.-C. Hsiao, S.-Y. Yang, B.-S. Lin, I.-J. Lee, and W. Chou, "Data glove embedded with 9-axis IMU and force sensing sensors for evaluation of hand function," in *Proc. IEEE EMBC*, Milan, Italy, Aug. 2015, pp. 4631–4634.

[18] H. G. Kortier, H. M. Schepers, and P. H. Veltink, "Identification of object dynamics using hand worn motion and force sensors," *Sensors*, vol. 16, no. 12, p. 2005, 2016.

[19] H. Liu *et al.*, "A glove-based system for studying hand-object manipulation via joint pose and force sensing," in *Proc. IEEE IROS*, Vancouver, BC, Canada, Sep. 2017, pp. 6617–6624.

[20] (2018). *FlexiForce A101 Sensor Datasheet Tekscan*. Boston, MA, USA. Accessed: May 28, 2019. [Online]. Available: https://www.tekscan.com/sites/default/files/resources/FLX-A101-F-Redesign_0.pdf

[21] M. Ferguson-Pell, S. Hagisawa, and D. Bain, "Evaluation of a sensor for low interface pressure applications," *Med. Eng. Phys.*, vol. 22, no. 9, pp. 657–663, 2000.

[22] G. De Pasquale, L. Mastrototaro, L. Pia, and D. Burin, "Wearable system with embedded force sensors for neurologic rehabilitation trainings," in *Proc. IEEE DTIP*, Roma, Italy, May 2018, pp. 1–4.

[23] M. J. Caruso, "Applications of magnetoresistive sensors in navigation systems," SAE Tech. Paper, Jan. 1997, pp. 15–21, vol. 72.

[24] S. O. H. Madgwick, A. J. L. Harrison, and R. Vaidyanathan, "Estimation of IMU and MARG orientation using a gradient descent algorithm," in *Proc. IEEE ICORR*, Zurich, Switzerland, Jul. 2011, pp. 1–7.

[25] J. Diebel, *Representing Attitude: Euler Angles, Unit Quaternions, and Rotation Vectors*. Stanford, CA, USA: Stanford Univ., 2006.

[26] J. R. Cook, N. A. Baker, R. Cham, E. Hale, and M. S. Redfern, "Measurements of wrist and finger postures: A comparison of goniometric and motion capture techniques," *J. Appl. Biomech.*, vol. 23, no. 1, pp. 70–78, Dec. 2007.

[27] K. N. Bachus, A. L. DeMarco, K. T. Judd, D. S. Horwitz, and D. S. Brodke, "Measuring contact area, force, and pressure for bioengineering applications: Using fuji film and TekScan systems," *Med. Eng. Phys.*, vol. 28, no. 5, pp. 483–488, 2006.

[28] S. Glowinski, A. Blazejewski, and T. Krzyzynski, "Human gait feature detection using inertial sensors wavelets," in *Wearable Robotics: Challenges Trends*. Berlin, Germany: Springer, 2016, pp. 397–401.

Bor-Shing Lin (M'01) received the B.S. degree in electrical engineering from National Cheng Kung University, Taiwan, in 1997, and the M.S. and Ph.D. degrees in electrical engineering from National Taiwan University, Taiwan, in 1999 and 2006, respectively.

He was the Principal Engineer of MStar Semiconductor from December 2007 to June 2009. Since 2009, he has been an Assistant Professor with the Department of Computer Science and Information Engineering, National Taipei University, Taiwan, where he is currently a Professor with the Department of Computer Science and Information Engineering. He is also the Vice Dean of College of EECS, National Taipei University. His research interests are in the areas of smart medicine, embedded system, wearable system, biomedical signal processing, biomedical image processing, and portable biomedical electronic system design.

I-Jung Lee (GS'15) received the B.S. degree in computer science and information engineering from National Taipei University, New Taipei City, Taiwan, in 2014, where she is currently pursuing the Ph.D. degree with the College of Electrical Engineering and Computer Science. Her research interests are in the areas of embedded systems and wearable devices applied to biomedical engineering.

Jean-Lon Chen was born in Taiwan, in 1971. He received the B.S. degree in medicine from China Medical University, Taiwan, in 1996, and the Ph.D. degree in psychology from the Goldsmiths College, University of London in 2013.

From 1998 to 2002, he was a Medical Doctor and a Resident Physician with the Department of Physical Medicine and Rehabilitation, Chang Gung Memorial Hospital. Since 2003, he has been an Attending Physician and an Academic Assistant Professor with the Department of Physical Medicine and Rehabilitation, Chang Gung Memorial Hospital. He has also been an Assistant Professor with the Medical Department, Chang Gung University, since 2006. He has published more than 30 articles. He holds one patent. His research interests include independent component analysis (ICA), EEG and event related potentials (ERPs), resting state networks (RSNs) and functional connectivity, neurofeedback training (NFT), stroke and traumatic brain injury, brain mapping and motor control, virtual reality, gerontology, acupuncture, and repetitive TMS applications.

Dr. Chen is an Associate Editor of the Taiwan *Journal of Physical Medicine and Rehabilitation*. He is also a Gerontologist and an Acupuncturist in Taiwan.